Analytical and Bioanalytical Chemistry (2021) 413:3529–3540
https://doi.org/10.1007/s00216-021-03304-9

RESEARCH PAPER

Polyethyleneimine-functionalized Fe_3O_4/attapulgite particles for hydrophilic interaction-based magnetic dispersive solid-phase extraction of fluoroquinolones in chicken muscle

Xiangdong Li[1] · Yihui Chen[2] · Shubing Chen[2] · Chunyan Hou[3] · Rongrong Xuan[4] · Yajie Gao[4] · Shuaijun Ren[4] · Lihui Yao[1] · Tingting Wang[1] · Lihua Zhang[3] · Yukui Zhang[3]

Received: 6 January 2021 / Revised: 12 March 2021 / Accepted: 19 March 2021 / Published online: 4 April 2021
© Springer-Verlag GmbH Germany, part of Springer Nature 2021

Abstract

Fluoroquinolone (FQ) residues in foods of animal origin may threaten public health but are challenging to determine because of their low contents and complex matrices. In this study, novel polyethyleneimine-functionalized Fe_3O_4/attapulgite magnetic particles were prepared by a simple co-mixing method and applied as hydrophilic sorbents for the magnetic dispersive solid-phase extraction (MSPE) of three FQs, i.e., ciprofloxacin, norfloxacin, and enrofloxacin, from chicken muscle samples. The preparation of the magnetic particles was of high reproducibility and the products could be reused many times with high adsorption capacity. The key experimental factors possibly influencing the extraction efficiencies, including sample solution, extraction time, sample loading volume, desorption solution, desorption time, and elution volume were investigated. Under optimum MSPE conditions, the analytes in chicken muscle samples were extracted and then determined by RPLC-MS/MS in MRM mode. Good linearity was obtained for the analytes with correlation coefficients ranged from 0.9975 to 0.9995. The limits of detection were in the range of 0.02–0.08 μg kg^{-1}, and the recoveries of the spiked FQs in chicken muscle samples ranged from 83.9 to 98.7% with relative standard deviations of 1.3–6.8% ($n = 3$). Compared with the traditional MSPE methods based on hydrophobic mechanism, this hydrophilic interaction-based method significantly simplifies the sample pretreatment procedure and improves repeatability. This method is promising for accurate monitoring of FQs in foods of animal origin.

Keywords Attapulgite · Fluoroquinolones (FQs) · Hydrophilic interaction · Magnetic dispersive solid-phase extraction (MSPE)

Introduction

Fluoroquinolones (FQs) are polar and zwitterionic molecules [1], including ciprofloxacin (CIP, pK_{a1} 6.1, pK_{a2} 8.7, octanol/water partition coefficient log P −1.70) [2, 3], norfloxacin (NOR, pK_{a1} 6.2, pK_{a2} 8.7, log P −2.00) [3, 4], and enrofloxacin (ENR, pK_{a1} 6.03, pK_{a2} 8.3, log P 1.88) [5, 6] (see Supplementary Information (ESM) Fig. S1), etc. FQs are widely used as feed additives in factory farms to prevent the spread of infectious diseases in crowded living conditions. Besides, the use of low and sub-therapeutic doses of FQs as growth promoters enhances livestock production [1]. However, the overuse of FQs in animal husbandry threatens public health because of the excess accumulation of FQ residues in food products. As antimicrobial resistance is becoming a global threat [7], it is necessary to keep the FQ residues in food products under frequent monitoring [8].

Nevertheless, it is challenging to determine FQ residues in foods of animal origin because of their low contents and complex matrices. Many sample preparation methods have been developed to extract and purify FQs from food samples, e.g., immunoaffinity extraction/microextraction [9, 10], matrix solid-phase dispersion (MSPD) [11–13], solid-phase microextraction (SPME) [14, 15], stir bar sorptive extraction

✉ Tingting Wang
shiming-49@163.com

[1] School of Materials and Chemical Engineering, Ningbo University of Technology, Ningbo 315211, China

[2] Ningbo Academy of Inspection and Quarantine, Ningbo 315012, China

[3] Key Laboratory of Separation Science for Analytical Chemistry, National Chromatographic Research and Analysis Center, Dalian Institute of Chemical Physics, Chinese Academy of Sciences, Dalian 116023, China

[4] The Affiliated Hospital of Medical School of Ningbo University, Ningbo 315020, China

[16], dispersive liquid–liquid microextraction [17, 18], QuEChERS (quick, easy, cheap, effective, rugged, and safe) approach [19], and solid-phase extraction (SPE) [20, 21]. Among them, the traditional SPE and the SPE-related methods such as MSPD are widely used. However, they are time-consuming and laborious, because the sorbents (and the samples of MSPD) packed in cartridges may result in column blocking, high backpressure, and limitation of the diffusion and the mass transfer rates. Besides, the packed column is usually utilized only once, especially for MSPD. To overcome the disadvantages, one solution is the magnetic dispersive solid-phase extraction (MSPE) method with magnetically separable sorbents. In typical MSPE, magnetic sorbents are dispersed in the sample solution and separated by an external magnet. The contact area between the sorbents and the analytes is increased, leading to improved mass transfer and extraction efficiency. Without column packing, the extraction procedure is simplified and the magnetic sorbents can be easily reused. These advantages make MSPE a promising technique for sample preparation [22–29].

In recent years, many efforts have been made to develop magnetic sorbents applied in flame retardancy [30], photocatalysis [31, 32], oil/water separation [33], etc. Various types of magnetic sorbents have also been explored for food analysis, e.g., magnetic graphene [22], Zr–Fe–C magnetic nanoparticles [23], one-dimensional polyaniline/magnetic nanoparticles [24], magnetic nanoparticles modified with polydimethylsiloxane and multiwalled carbon nanotubes (magnetic PDMS/MWCNTs-OH particles) [25], Fe_3O_4@MCM-48 nanocomposite [26], Fe_3O_4@SiO_2 microspheres with phenyl and tetrazolyl groups (Fe_3O_4@SiO_2@TZ@Ph magnetic microspheres) [27], magnetic molecularly imprinted polymers [28], and surface-imprinted magnetic carboxylated cellulose nanocrystals (Fe_3O_4@CCNs@MIPs) [29]. The adsorption of these sorbents was mainly based on hydrophobic interaction. The extracts had to be dried and re-dissolved in a more polar solvent (e.g., water) before separated by reversed-phase liquid chromatography (RPLC) [22, 24–29]. As a result, the error of determination, as well as the time for sample pretreatment, might increase. In contrast to the hydrophobic sorbents, hydrophilic sorbents are eluted by aqueous solutions or low-concentrated organic solvents compatible with the following RPLC. Additionally, since the real samples are commonly treated by high-concentrated organic solvents (e.g., ACN) before SPE, the resultant organic phase can be loaded directly to hydrophilic sorbents, further simplifying the pretreatment procedure. However, there has been no report upon the MSPE method based on hydrophilicity to the best of our knowledge.

Attapulgite (ATP) is a low-cost natural nanostructural fibrillar material with large surface area, porous structure, adjustable surface chemistry, and cation exchange capacity. In our previous work, it was introduced to monoliths to improve the adsorption capacity and separation efficiency of hydrophilic analytes [34, 35]. In this study, ATP and a cationic polymer, polyethyleneimine (PEI), were used to prepare hydrophilic PEI-functionalized Fe_3O_4/ATP magnetic particles. The developed hydrophilic magnetic particles were applied as MSPE sorbent for the determination of three FQs in chicken muscle samples. The particles were characterized by scanning electron microscopy/energy dispersive analysis of X-ray (SEM/EDAX), transmission electron microscopy (TEM), Fourier transform infrared spectroscopy (FTIR), vibrating sample magnetometer (VSM), and X-ray diffraction (XRD). The main factors affecting the extraction efficiency, i.e., sample solution, extraction time, sample loading volume, desorption solution, desorption time, and elution volume, were systematically investigated as well.

Material and methods

Reagents and materials

PEI (hyperbranched, M.W. 1800, 99.0%), iron (III) chloride hexahydrate ($FeCl_3 \cdot 6H_2O$, ≥ 99.0%), iron (II) sulfate heptahydrate ($FeSO_4 \cdot 7H_2O$, ≥ 99.0%), formic acid (LC-MS grade, 99.0%), and KBr (FTIR grade, > 99.5%) were purchased from Aladdin (Shanghai, China). HPLC-grade ACN was obtained from Tedia (Fairfield, OH, USA). $NH_3 \cdot H_2O$ (25%), hydrochloric acid (37%), NaCl (99.5%), anhydrous sodium sulfate (99.0%), and sodium hydroxide (96%) were purchased from Sinopharm Chemical Reagent Co., Ltd. (Beijing, China). Natural ATP was provided by Jiangsu Xuyi Anhalt Nonmetallic Mining Ltd. (Jiangsu, China). All the FQ standards of CIP, ENR, and NOR were obtained from Aladdin (Shanghai, China). Ultra-pure water was produced by a Milli-Q system (Millipore, Molsheim, France). ProMax syringe filters (13 mm, 0.22 μm nylon) were supplied by Dikma (Beijing, China).

Stock solutions (1.0 mg mL^{-1}) of FQ standards were prepared in ACN and stored at 4 °C before use. Working standards with specific concentrations for MSPE optimization were prepared daily by diluting a mixture of the stock solutions.

Characterization

FTIR spectra were obtained on a Bruker MPA FTIR spectrometer (Bremen, Germany) using KBr pellets in the range of wave number 400–4000 cm^{-1}. The SEM images and EDAX spectra were acquired using a Hitachi S-4800 scanning electron microscope (Tokyo, Japan). The morphology of PEI-functionalized Fe_3O_4/ATP magnetic particles was analyzed by a Lorentz-TEM (JEM-2100F, Japan). The XRD patterns were recorded on a Bruker AXS D8 Advance X-ray

diffractometer using Ni-filtered Cu Kα radiation (Karlsruhe, Germany). The magnetic properties were measured at room temperature using a VSM (Lake Shore 7410, Columbus, USA) in an applied magnetic field sweeping between ± 20,000 Oe.

Preparation of the magnetic dispersive solid-phase extraction sorbent

The natural ATP was acidified by hydrochloric acid before use according to our previous method [36]. In a typical procedure, 1.46 g of $FeSO_4 \cdot 7H_2O$, 2.13 g of $FeCl_3 \cdot 6H_2O$, 0.6 g of acidified ATP, and 0.15 g of PEI were ultrasonically dispersed in 60 mL of water for 70 min. Subsequently, the homogeneous yellow solution was added with 5 mL of $NH_3 \cdot H_2O$ and stirred at 70 °C for 1.5 h until black magnetite particles were formed. The black products were collected by magnetic separation, then washed to neutral with ultrapure water, and finally dried at 70 °C for 6 h.

Real sample preparation

Chicken muscle samples were obtained from a local supermarket (Ningbo, China) and stored at − 20 °C before use. Briefly, appropriate volumes of working solutions of FQ standards were added into 5.0 g minced chicken muscle samples. After that, 30 g anhydrous sodium sulfate was added, as well as 25 mL acidified ACN consisting of 6 mol L^{-1} hydrochloric acid-ACN (1:125, v/v). The mixture was homogenized and mechanically shaken for 15 min, transferred to a 50-mL polypropylene tube, and centrifuged at 4500 r min^{-1} for 15 min. The supernatant was moved to a 50-mL volumetric flask, while another 20 mL of acidified ACN was added to the residue which went through the above operations for a second time. The supernatant was combined, and 2.5 mL of water was added. The pH of the resulting solution was adjusted to neutral with sodium hydroxide. Finally, the mixture in the 50-mL volumetric flask was diluted to the mark with ACN for the subsequent MSPE procedure. The final volume percentage of ACN in this mixture was about 95%.

Hydrophilic interaction-based magnetic dispersive solid-phase extraction

The above sample extract (10.0 mL) and 50.0 mg of PEI-functionalized Fe_3O_4/ATP magnetic particles were mixed in a 15-mL vial under the ultrasonic condition at 15 °C for 20 min to allow the targets trapped by the MSPE sorbents. After that, the magnetic sorbents with FQs were isolated from the solution by an external magnet. The elution was carried out with 0.5 mL of 4.6 wt% $NH_3 \cdot H_2O$ aqueous solution containing 160 mM NaCl (pH 12.23) under the ultrasonic condition at 30 °C for 10.0 min. With the help of a magnet, the eluate was collected and adjusted to neutral with hydrochloric acid. Finally, the solution was filtered and then injected directly into RPLC-MS/MS system for subsequent analysis.

Evaluation of adsorption capacity

The adsorption capacity of the magnetic particles was evaluated as described previously with a minor modification [37]. In brief, 1.0 mL of NOR at various concentrations in 95% (v/v) ACN was loaded onto 50 mg of hydrophilic magnetic particles with or without ATP, followed by the elution with 1.0 mL of 4.6 wt% $NH_3 \cdot H_2O$ aqueous solution containing 160 mM NaCl (pH 12.23). At last, the eluate was filtered and injected into the RPLC-UV system for analysis.

RPLC-UV and RPLC-MS/MS conditions

For the optimization and evaluation of the MSPE based on the developed magnetic sorbent, the eluate was analyzed by RPLC-UV which was carried out on an Ultimate 3000 LC system consisting of an autosampler, a UV detector, a vacuum degasser, a column oven, a quaternary pump, and a data acquisition module (Dionex, Sunnyvale, CA, USA). The RPLC separation was conducted in an Agilent InfinityLab Poroshell 120 EC-C18 column (150 mm × 4.6 mm, 4.0 μm) at a flow rate of 0.8 mL min^{-1}. The mobile phase was 10% buffer (10 mM ammonium formate adjusted to pH 3.0 with formic acid)-90% ACN. The injection volume was 20 μL, and the temperature of the column oven was set at 30 °C. The wavelength for UV detection was set at 280 nm. Baseline separation of the three FQs was completed within 6 min.

The method validation and application for FQs determination were performed on a triple quadrupole mass spectrometer (MS/MS, AB4000 QTRAP, AB SCIEX, Ontario, Canada) coupled to a Shimadzu HPLC system (LC-20AD, Kyoto, Japan). Three FQs were separated by an Agilent XDB C18 column (150 mm × 4.6 mm, 5 μm). The binary mobile phases were 0.1% formic acid in ACN (A) and 0.1% formic acid in water (B). The linear gradient elution mode was as follows: 0.00–6.00 min = 95% B to 0% B, 6.00–11.00 min = 0% B, 11.00–11.20 min = 0% B to 95% B, and 11.20–15.00 min = 95% B. The column temperature, the flow rate, and the injection volume were 30 °C, 0.8 mL min^{-1}, and 20 μL, respectively. The mass spectrometer was operated in positive electrospray ionization (ESI) and multiple reaction monitoring (MRM) modes. The source temperature and the ESI voltage were 550 °C and 5500 V, respectively. Nitrogen was adopted as the ion source nebulizing gas (gas 1, 50 psi) and the auxiliary gas (gas 2, 50 psi). Table S1 (see the ESM) shows the MRM transitions (precursor ions → product ions) and collision energies. Note that although the analytes present different log *P* values, they are ionized in the RPLC mobile phase (pH 3.00), leading to similar retention times.

Results and discussion

Preparation of the polyethyleneimine-functionalized Fe_3O_4/attapulgite magnetic particles

Novel PEI-functionalized Fe_3O_4/ATP magnetic particles were prepared by a simple co-mixing method. The mass ratio of $FeCl_3{\cdot}6H_2O$ to ATP in the initial mixture was optimized with the ratio of $FeCl_3{\cdot}6H_2O/FeSO_4{\cdot}7H_2O$ kept consistent. ATP is completely magnetized when the mass ratio of $FeCl_3{\cdot}6H_2O$ to ATP is 3.55 (see ESM Fig. S2A). With a ratio of 2.34, only some of the particles are attracted to the magnet (see ESM Fig. S2B), while no magnetic particles are formed on the surface of ATP with even lower ratios. The reason may be attributed to the adsorption of cations on the surface of ATP. In the initial aqueous solution, Fe^{2+} and Fe^{3+} will be adsorbed to the negative centers on the surface of ATP introduced by the hydrochloric acid treatment. When $NH_3{\cdot}H_2O$ (pH 11.41) is added, Fe_3O_4 particles will be formed by coprecipitation. If the Fe^{3+} and Fe^{2+} in the initial mixture are not sufficient, they will be completely adsorbed on the ATP surface, with little iron ions to form Fe_3O_4 particles. Therefore, $FeCl_3{\cdot}6H_2O$ and ATP with a mass ratio of 3.55 were used for sorbent preparation.

Besides, PEI in the initial mixture will be partially protonated when $NH_3{\cdot}H_2O$ (pH 11.41) is added, because the pK_a values of the primary, secondary, and tertiary amine groups of PEI are 4.5, 6.7, and 11.6, respectively [38]. Considering the isoelectric point of the naked Fe_3O_4 of about 6.7 [39], PEI cations will be adsorbed on the surface of ATP and naked Fe_3O_4 particles. Thus, PEI has been added to the initial mixture to improve the hydrophilicity of the developed particles. The ratio of ATP to PEI was based on our previous work [40].

Characterization of the polyethyleneimine-functionalized Fe_3O_4/attapulgite magnetic particles

The FTIR spectra of naked Fe_3O_4, acidified ATP, and PEI-functionalized Fe_3O_4/ATP magnetic particles are presented in Fig. S3 (see the ESM). A strong absorption band at 578 cm^{-1} is assigned to the Fe–O vibration of magnetite [41], appearing in the FTIR spectra of the naked Fe_3O_4 particles (see ESM Fig. S3A) and the PEI-functionalized Fe_3O_4/ATP magnetic particles (see ESM Fig. S3C). Two intense absorption bands located at 3545 and 3412 cm^{-1} are attributed to the stretching vibrations of the Al–OH and Fe–OH groups [42], respectively, appearing in the FTIR spectra of acidified ATP (see ESM Fig. S3B) and PEI-functionalized Fe_3O_4/ATP magnetic particles (see ESM Fig. S3C). Besides, the bands at 1026 and 470 cm^{-1} correspond to the stretching vibrations of Si–O–Si bonds [43]. In addition, a new peak at 1462 cm^{-1} due to the coupling of C–N stretching vibrations and the N–H angular deformation is presented in the FTIR spectrum of PEI-functionalized Fe_3O_4/ATP magnetic particles (Fig. S3C) [40]. Furthermore, there is a band at 1360 cm^{-1} which is associated with the C–N stretching vibration of the tertiary amine [44]. These results demonstrate that the PEI-functionalized Fe_3O_4/ATP magnetic particles have been prepared successfully.

Morphologies of acidified ATP and PEI-functionalized Fe_3O_4/ATP magnetic particles are shown in SEM (Fig. 1) and TEM images (see ESM Fig. S4). As shown in Fig. 1a, the acidified ATP is in the form of separate fibers. It can be seen in Fig. 1b and Fig. S4 (see the ESM), the surface of PEI-functionalized Fe_3O_4/ATP magnetic particles has a layer of granular material, indicating that the ATP provides stable anchoring sites for the deposition of Fe_3O_4 particles. Furthermore, the elemental compositions (except carbon) of the acidified ATP (Fig. 1a) and the PEI-functionalized Fe_3O_4/ATP magnetic particles (Fig. 1b) were determined by EDAX. The former is composed primarily of oxygen, magnesium, aluminum, silicon, and iron, while the latter is primarily nitrogen, oxygen, magnesium, aluminum, silicon, and iron. The distinctive nitrogen element is attributed to the presence of PEI. Besides, the increased content of iron indicates that the magnetic particles have been trapped on the surface of ATP.

Since magnetization was crucial for MSPE operation, the magnetic hysteresis loops of naked Fe_3O_4 and PEI-functionalized Fe_3O_4/ATP were measured by VSM at room temperature. The saturation magnetization values are found to be 77.1 and 48.6 emu g^{-1}, respectively (see ESM Fig. S5A). A reduction of ~ 37% resulted from the combination of ATP, PEI, and Fe_3O_4. This phenomenon may be attributed to the surface effect on small particles, the increased surface disorder, and the diamagnetic contribution of ATP and PEI. Nevertheless, the magnetism of the PEI-functionalized Fe_3O_4/ATP particles is sufficient for magnetic separation.

The XRD pattern of PEI-functionalized Fe_3O_4/ATP is illustrated in Fig. S5B (see the ESM). Six characteristic peaks of Fe_3O_4 observed at $2\theta =$ 30.21°, 35.62°, 43.27°, 53.44°, 57.17°, and 62.84° are indexed to the (220), (311), (400), (422), (511), and (440) crystal planes, respectively. The results are in agreement with that of magnetite (JCPDS powder diffraction data file No. 79-0418), indicating that the structure of Fe_3O_4 has remained the same during the functionalization process.

Optimization of magnetic dispersive solid-phase extraction conditions

Standard solutions of CIP, ENR, and NOR each at 0.01 mg mL^{-1} were used for MSPE optimization. The volume percentage of ACN, a common organic solvent for HILIC SPE, in the solution varied from 0 to 95%. The corresponding recoveries are compared as shown in Fig. 2. The recoveries remained almost unchanged until the ACN content reached 90% and increased sharply with the increase of ACN content

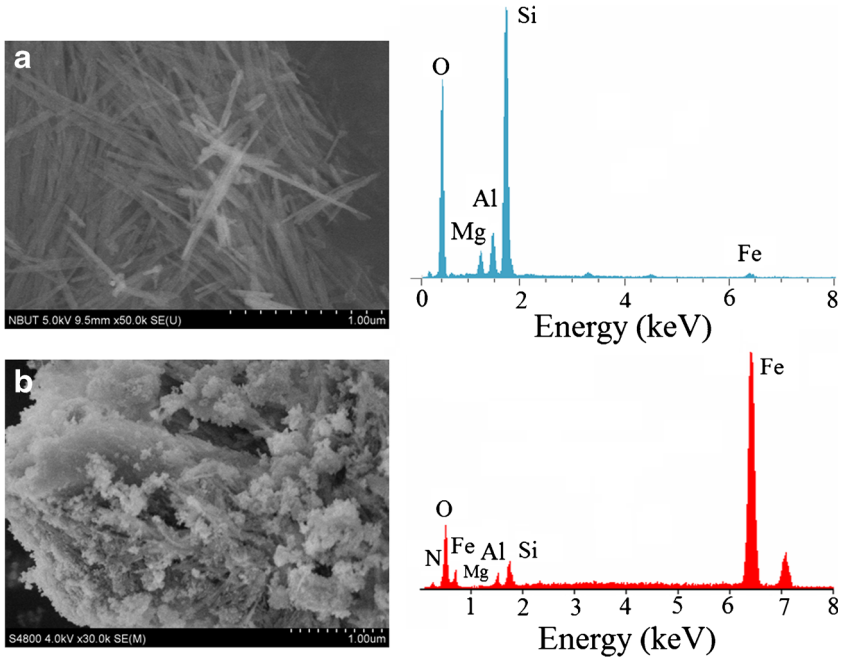

Fig. 1 SEM images and EDAX spectra of acidified ATP (**a**) and PEI-functionalized Fe_3O_4/ATP magnetic particles (**b**)

from 90 to 95%. This interesting phenomenon is consistent with the HILIC separation mechanism [45], indicating that the interaction between three targets and PEI-functionalized Fe_3O_4/ATP particles is mainly hydrophilic. Since the maximum recoveries were obtained with 95% ACN, it was employed in the following experiments.

Salt in sample solution may affect the recoveries as well. In 95% ACN solution, the sodium sulfate added in the chicken muscle pretreatment step for dehydration is virtually insoluble. The solubility of other salts in such a highly concentrated organic solvent is also very low. The maximum concentration for NaCl in 95% ACN was found to be 100 mM, and its effect was investigated. The recoveries of NOR, CIP, and ENR in 95% ACN with or without 100 mM NaCl were 101.0%, 86.1%, 84.5% and 101.5%, 89.3%, 84.1%, respectively.

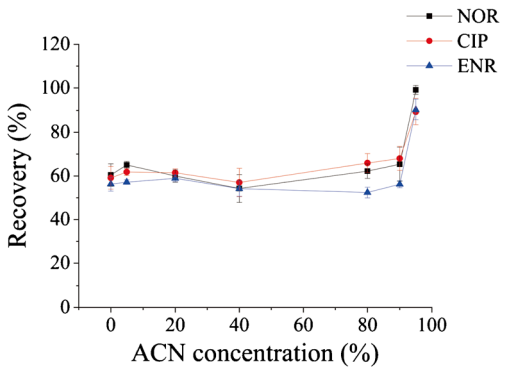

Fig. 2 Effect of ACN concentration on recoveries of FQs. The concentration of each FQ was 0.01 mg mL^{-1}. The elution solution was 4.6 wt% $NH_3 \cdot H_2O$ aqueous solution. Both extraction time and desorption time were 10 min. The ultrasonic bath temperatures for adsorption and desorption were both 25 °C. The sample loading and elution volumes were 1.0 mL

Since the salt showed little impact on the recoveries, it was omitted to simplify the experimental procedure.

Magnetic extraction is generally carried out at room temperature (~ 25 °C), which can be sped up by ultrasound [46]. Under such conditions, the recoveries of NOR, CIP, and ENR were 81.4%, 82.1%, and 77.2%, respectively. When the temperature of the ultrasonic bath was lowered to about 15 °C by ice bags, the recoveries increased to 103.5%, 93.4%, and 96.1%, respectively. At this temperature, the maximum recoveries were reached after 20 min (see ESM Fig. S6). Hence, the ultrasound-assisted magnetic extraction was performed in a water bath at 15 °C for 20 min in the following experiments.

The effect of ultrasonic bath temperature (i.e., 25, 30, and 40 °C) on the recoveries during the desorption procedure was also investigated (data not shown). The recoveries were positively correlated with the temperature in a range from 25 to 30 °C. The increase in recoveries can be ascribed to the cavitation bubbles, which are more likely to be produced at a higher temperature thanks to lower liquid viscosity and tensile stress. With the temperature further increasing from 30 to 40 °C, no obvious changes were observed in the recoveries, indicating that most of the targets had already been desorbed from the PEI-functionalized Fe_3O_4/ATP magnetic particles. Thus, 30 °C was chosen as the ultrasonic bath temperature in the desorption step for the subsequent studies.

The pH of the desorption solvent is a crucial factor that determines the existing forms of the targets and the surface charge of the PEI-functionalized Fe_3O_4/ATP magnetic particles. In our previous works, extremely acidic solvents were used to elute targets from PEI-modified sorbents [40, 47, 48]. However, the naked Fe_3O_4 particles are unstable and tend to be oxidized under extremely acidic conditions [49].

Accordingly, the alkaline solvent was used for desorption. We compared the recoveries obtained by 5 mM ammonium formate with pH values between 8.00 and 12.00 adjusted by $NH_3 \cdot H_2O$, as well as an aqueous solution of 4.6 wt% $NH_3 \cdot H_2O$ at an even higher pH of 12.23 (Fig. 3). Theoretically, under the alkaline condition, the tertiary amine groups ($pK_a \sim 11.6$) and the secondary amine groups ($pK_a \sim 6.7$) of PEI will partially carry positive charges, while the primary amines ($pK_a \sim 4.5$) of PEI are in the form of neutral molecules [38]. Therefore, with the increase of the pH from 8.00 to 12.23, the positive charges on the surface of PEI-functionalized Fe_3O_4/ATP will decrease. NOR, CIP, and ENR, with the pK_{a1}/pK_{a2} values of 6.2/8.7, 6.1/8.7, and 6.03/8.3, respectively, will be partially deprotonated and partially in neutral forms over a pH range of 8.00 to 11.00 ($pK_{a1} + 2$), and will be completely negatively charged when pH > 11 ($pK_{a2} + 2$). The negative charges of the targets can interact with the positive charges on the PEI-functionalized Fe_3O_4/ATP by electrostatic interaction, while the targets in the neutral form can interact with the natural form of the amine groups on the sorbent surface by hydrogen bonding. It was found that with an increase of the pH value from 8.00 to 11.00, the recoveries of all targets increased. Because the targets became more negatively charged and the developed sorbent was less positively charged, leading to a reduction of the electrostatic interaction and the hydrogen bonding. However, when the pH value further increased, the recoveries of the three targets changed differently. The reason may be ascribed to different interaction mechanisms based on their molecular structures (see ESM Fig. S1). ENR contains both cyclopropyl group and ethyl group, while CIP contains a cyclopropyl group and NOR has an ethyl group. The cyclopropyl group enhances electrostatic interaction but inhibits hydrogen bonding, while the ethyl group on the contrary. For ENR and CIP, the major interaction to the sorbent is electrostatic interaction which will decrease when the pH value increased from 11.00 to 12.00, leading to an increase in their recoveries. However, the main interaction between NOR and PEI-functionalized Fe_3O_4/ATP magnetic particles is hydrogen bonding when pH > 11.00. Therefore, the charge state of the sorbent had a slight impact on the recovery of NOR at pH 11.00–12.00. When 4.6 wt% $NH_3 \cdot H_2O$ (pH 12.23) was used instead of 5 mM ammonium formate, ENR and NOR could form strong hydrogen bonding with $NH_3 \cdot H_2O$, resulting in the recovery increase. However, the recovery of CIP obtained with 4.6 wt% $NH_3 \cdot H_2O$ (pH 12.23) was similar to that obtained with 5 mM ammonium formate at pH 12.00. The reason may be ascribed to the cyclopropyl group of CIP. At pH 12.23, the electrostatic interaction could be still playing a major role and the increase of pH from 12.00 to 12.23 had little impact on the recovery of CIP. Since satisfactory recoveries for all three targets were obtained at pH 12.23, the aqueous solution of 4.6 wt% $NH_3 \cdot H_2O$ was chosen for further optimization.

The effect of salt in desorption solution was studied via varying the NaCl concentration in 4.6 wt% $NH_3 \cdot H_2O$ from 0 to 160 mM. The recoveries of the three analytes decrease with an increasing salt concentration to 4 mM, followed by an increase at higher salt concentrations (Fig. 4). The partitioning model for HILIC assumes the presence of a water-rich liquid layer on the sorbent surface [45]. Higher salt concentration will drive more solvated salt ions into this layer, thus increasing its volume or hydrophilicity, leading to strong retention and reduced recoveries of the analytes [50]. However, when the salt concentration further increases, the electrostatic interaction is more notable than the hydrophilic interaction [51]. Therefore, the recoveries increased accordingly. Besides, more salt was found to be beneficial to magnetic separation. Hence, further experiments were carried out with 160 mM of NaCl in the desorption solvent.

The effect of desorption time on the recoveries of FQs was also studied. With ultrasonic assistance, 10 min is found to be suitable for desorption as shown in Fig. S7 (see the ESM). A slight drop in the recoveries is observed with a longer desorption time, which is consistent with the previous reports [25, 28]. The reason can be the reversible adsorption to some degree during the excessive time.

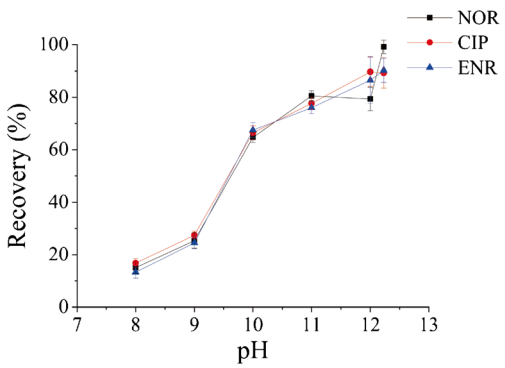

Fig. 3 Effect of pH on recoveries of FQs. Each FQ was prepared in 95% (v/v) ACN/H_2O at a concentration of 0.01 mg mL^{-1}. The extraction time and desorption were 20 min and 10 min, respectively. The ultrasonic bath temperatures for adsorption and desorption were 15 °C and 30 °C, respectively. The sample loading and elution volumes were 1.0 mL

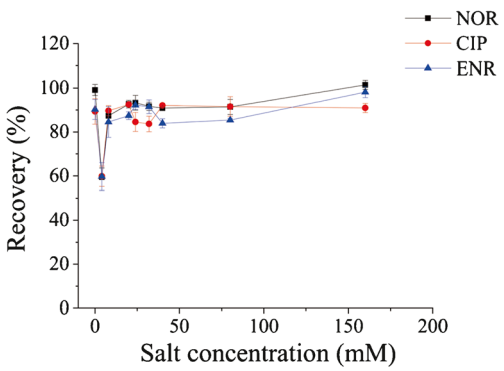

Fig. 4 Effect of salt concentration on recoveries of FQs. Other conditions were the same as those in Fig. 3

Table 1 Within-batch and batch-to-batch precisions of the preparation of PEI-functionalized Fe_3O_4/ATP magnetic particles as hydrophilic MSPE sorbent ($n = 3$)

Analyte	Within-batch		Batch-to-batch	
	Recovery (%)	RSD (%)	Recovery (%)	RSD (%)
NOR	101.5	2.1	99.9	3.3
CIP	91.0	2.1	90.7	2.3
ENR	98.2	2.5	91.0	4.9

Additionally, the effect of sample loading volume on the recoveries is illustrated in Fig. S8 (see the ESM). Higher recoveries (> 85%) were achieved with loading volumes of 1.0–10.0 mL. Further increase of the volume led to an obvious decrease in recoveries. As a result, 10.0 mL of sample loading volume was implemented in the subsequent experiments.

The effect of desorption volume on the recoveries was also evaluated (see ESM Fig. S9). With the increase of the volume from 0.2 to 0.5 mL then to 1.0 mL, the recoveries increased to a maximum and remained almost unchanged, indicating 0.5–1.0 mL of desorption solvent would be sufficient. When the volume increased from 1.0 to 3.0 mL, the recoveries of NOR and CIP remained the same, while that of the ENR slightly decreased. This phenomenon may be explained as follows. The large contact area between PEI-functionalized Fe_3O_4/ATP magnetic particles and analytes increases the possibility of reversible adsorption. Being more hydrophobic than NOR and CIP, ENR is more likely to interact with the reticulated carbon chains on the PEI-functionalized Fe_3O_4/ATP magnetic particles, resulting in a slight decrease in its recovery. Considering the recoveries and to obtain better detection limits, 0.5 mL of desorption solvent was adopted.

Reproducibility of sorbent preparation

Under the optimized conditions, the reproducibility of the preparation of PEI-functionalized Fe_3O_4/ATP magnetic particles is evaluated with the FQ recoveries (Table 1). The recoveries ranged from 91.0 to 101.5% with the relative standard deviations (RSDs) of 2.1–2.5% within one batch. The batch-to-batch recoveries ranged from 90.7 to 99.9% with the RSDs of 2.3–4.9%, demonstrating good reproducibility of the sorbent preparation and the robustness of the method.

Stability and reusability of the developed magnetic sorbent

As mentioned above, the optimum desorption solvent was 4.6 wt% $NH_3 \cdot H_2O$ aqueous solution containing 160 mM NaCl (pH 12.23), which was very alkaline and might affect the stability and the reusability of the developed magnetic sorbent. Therefore, successive MSPE tests were carried out. In each MSPE test, the PEI-functionalized Fe_3O_4/ATP magnetic particles were eluted by 0.5 mL of the optimum desorption

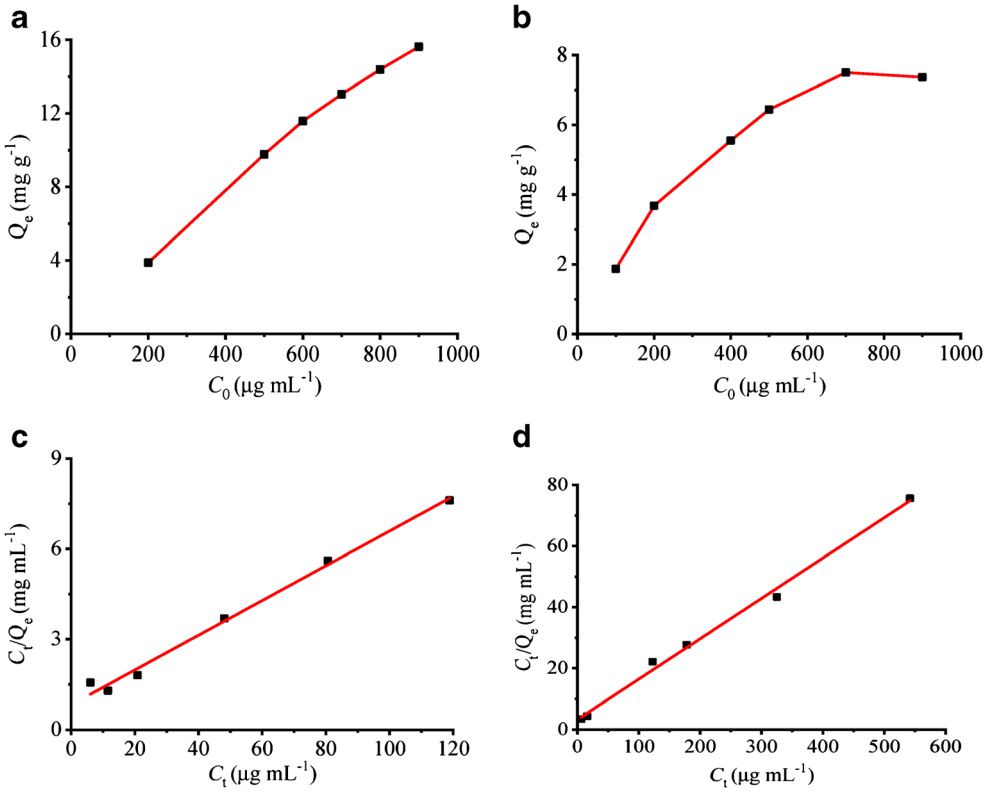

Fig. 5 Adsorption isotherms of NOR on the PEI-functionalized Fe_3O_4/ATP magnetic particles (**a**) and the PEI-functionalized Fe_3O_4 magnetic particles (**b**) and the related Langmuir adsorption models of NOR on the PEI-functionalized Fe_3O_4/ATP magnetic particles (**c**) and the PEI-functionalized Fe_3O_4 magnetic particles (**d**)

Table 2 Linear relationships, LODs, and LOQs of the FQs in chicken muscle samples obtained by MSPE coupled with RPLC-MS/MS ($n = 3$)

Analyte	Linear range (μg kg^{-1})	Regression equation	R^2	LOD (μg kg^{-1})	LOQ (μg kg^{-1})
NOR	0.05–100	y=80,056x+4679	0.9980	0.02	0.05
CIP	0.25–100	y=18,159x+1346	0.9975	0.08	0.25
ENR	0.20–100	y=23,107x+1656	0.9995	0.06	0.20

solvent, then washed with 38% (v/v) ACN in water until the solution pH became neutral. After that, the particles were dried for the next use. The RSDs of the peak areas of NOR, CIP, and ENR for 40 runs within 8 days were 4.1%, 5.6%, and 8.1%, respectively. The results demonstrate that the PEI-functionalized Fe_3O_4/ATP magnetic particles are stable in the alkaline desorption solvent and can be reused at least 40 times.

Adsorption capacity of the developed magnetic sorbent

The adsorption capacities of NOR on the PEI-functionalized Fe_3O_4/ATP magnetic particles and the PEI-functionalized Fe_3O_4 magnetic particles were compared to evaluate the effect of ATP. The amount of NOR adsorbed on the sorbent (Q_e, μg mg^{-1}) is calculated from the concentration of the eluate. Conversely, C_t is determined using the following equation:

$$C_t = C_0 - Q_e m/V \quad (1)$$

where C_0 and C_t are the initial and equilibrium concentrations (μg mL^{-1}) of NOR in solution, V is the volume (mL), and m is the mass (mg) of the hydrophilic magnetic particles [52].

The adsorption isotherms of NOR show that the adsorption amount of PEI-functionalized Fe_3O_4/ATP magnetic particles is far from the maximum (Fig. 5a) when the adsorption amount of PEI-functionalized Fe_3O_4 magnetic particles reaches a plateau of about 7.5 mg g^{-1} (Fig. 5b). The adsorption capacity is also estimated based on the Langmuir isotherm model [53]:

$$C_t/Q_e = C_t/Q_0 + 1/(K_L Q_0) \quad (2)$$

where Q_0 refers to the maximal adsorption capacity (mg g^{-1}), and K_L denotes the Langmuir isotherm constant (L mg^{-1}). As shown in Fig. 5c, d, good linear relationships between C_t/Q_e and C_t are presented with the correlation coefficients (R^2) > 0.99. For the PEI-functionalized Fe_3O_4 magnetic particles with a regression equation of $y = 0.132x + 3.211$ (y referring to C_t/Q_e and x to C_t), the maximal adsorption capacity was calculated to be 7.58 mg g^{-1} using the slope. It is consistent with the previous result obtained by the adsorption isotherm (Fig. 5b). For the PEI-functionalized Fe_3O_4/ATP magnetic particles with a regression equation of $y = 0.0577x + 0.822$, the maximal adsorption capacity was found to be 17.33 mg g^{-1}, significantly improved by ATP introduced to the magnetic particles. The reason may be that the acidified ATP bears three different types of water molecules (i.e., sorption water on the surface, zeolitic water in the micro-channel, and structural water) and reactive –OH groups, improving hydrophilic interaction between the sorbent and the analytes [34].

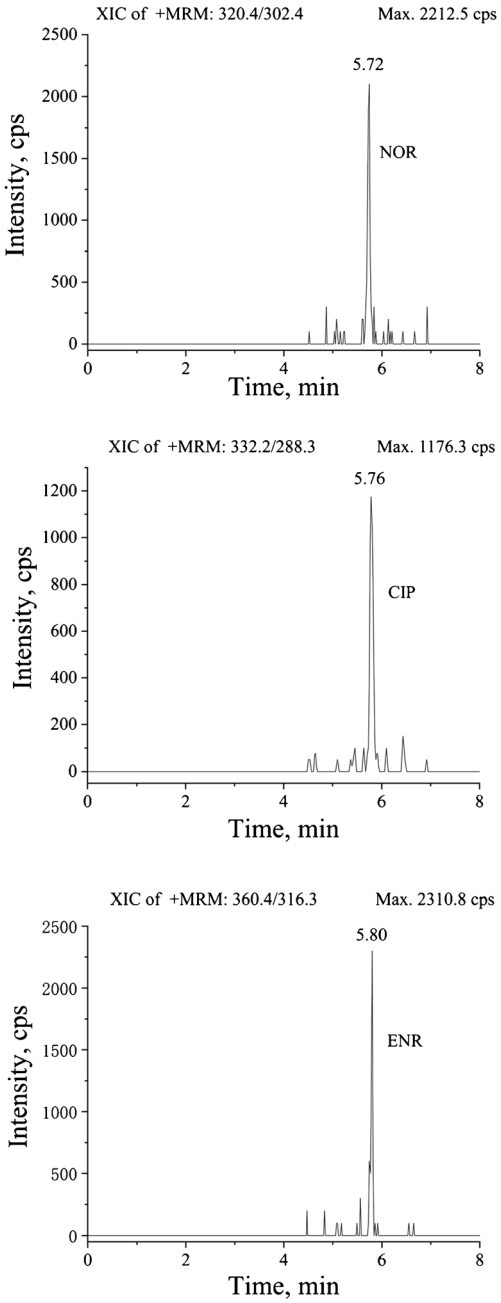

Fig. 6 Extracted ion chromatograms of NOR, CIP, and ENR in chicken muscle sample spiked at 0.05, 0.25, and 0.20 μg kg^{-1}, respectively

Method validation

The calibration curves were constructed by plotting the peak areas obtained by RPLC-MS/MS under MRM mode (i.e., *Y*, counts) against the spiked concentrations of the FQs in the blank matrix (i.e., *X*, μg kg^{-1}). As shown in Table 2, good linearity was achieved with R^2 ranging from 0.9975 to 0.9995. The limits of detection (LODs) and the limits of quantification (LOQs) were determined by decreasing the spiked concentrations of the FQs to signal-to-noise ratio of 3 and 10, respectively. As a result, the LODs and LOQs for NOR, CIP, and ENR were 0.02, 0.08, 0.06 μg kg^{-1} and 0.05, 0.25, 0.20 μg kg^{-1}, respectively. Figure 6 shows the typical extracted ion chromatograms of NOR, CIP, and ENR in blank chicken muscle sample spiked at 0.05, 0.25, and 0.20 μg kg^{-1}, respectively. The LOQs are far below the maximum residue limits defined in the Official Journal of the European Union (e.g., 100 μg kg^{-1} for ENR), demonstrating good sensitivity of this method.

To evaluate the matrix effect of real samples, calibration curves were established using standard FQ solutions. The FQs were dissolved in 95% (v/v) ACN at the same concentrations as those spiked in matrix-matched solutions (data not shown here). The slope ratios of the matrix-matched curves to the standard ones (i.e., in 95% ACN) for NOR, CIP, and ENR were calculated to be 1.07, 0.84, and 1.10, respectively. With the slope ratios between 0.8 and 1.2, the matrix effects are relatively tolerable [54]. Nevertheless, to obtain more reliable results, the matrix-matched calibration standard curves were used for the determination of FQs in real samples.

Application

Under the optimal conditions, the FQs spiked at three levels in chicken muscle samples were determined three times by the developed hydrophilic interaction-based MSPE method coupled with RPLC-MS/MS. The concentrations of NOR, CIP, and ENR in the studied original chicken muscle samples were lower than the LODs. The recoveries are calculated by the formula as follows:

$$\text{Recovery}\ (\%) = (C_{\text{found}} - C_{\text{real}})/C_{\text{spiked}} \times 100 \quad (3)$$

where C_{found}, C_{real}, and C_{spiked} are the quantity (μg kg^{-1}) of analyte recovered from the spiked sample, the quantity of analyte in the original chicken muscle sample, and the quantity of analyte added, respectively. As shown in Table 3, satisfactory recoveries between 83.9% and 98.7% are obtained with acceptable RSDs less than 6.8%. The results demonstrate that the proposed hydrophilic interaction-based MSPE method is selective, accurate, and reliable for real sample monitoring.

Comparison of the proposed method with other MSPE methods

To the best of our knowledge, this is the first study reporting the hydrophilic interaction-based MSPE method for the analysis of FQs in foods. Previously reported MSPE methods for FQ determination are mainly based on hydrophobicity (Table 4). Therefore, one or two extra drying steps are required, diminishing the repeatability. In contrast, the PEI-functionalized Fe_3O_4/ATP magnetic particles extract FQs based on hydrophilic mechanism, producing eluate compatible with the following RPLC. Therefore, the sample pretreatment procedure can be greatly simplified without those drying steps, leading to improved repeatability with better RSDs (Table 4). In addition, coupling the hydrophilic MSPE with RPLC-MS/MS provides excellent sensitivity with low LODs for the FQs in the real sample. It is demonstrated that this method is promising for accurate monitoring of FQs in food products.

Table 3 Recoveries and RSDs of the FQs spiked at three levels in chicken muscle samples ($n = 3$)

Analyte	C_{real} (μg kg^{-1})	C_{spiked} (μg kg^{-1})	C_{found} (μg kg^{-1})	Recovery (%)	RSD (%)
NOR	n.d.	2.5	2.333	93.3	3.2
		25	24.67	98.7	1.9
		100	97.50	97.5	3.3
CIP	n.d.	2.5	2.098	83.9	3.1
		25	23.22	92.9	1.3
		100	94.70	94.7	5.3
ENR	n.d.	2.5	2.155	86.2	6.8
		25	24.15	96.6	1.4
		100	92.20	92.2	5.4

n.d. not detected

Table 4 Comparison of the developed hydrophilic MSPE method with previously reported MSPE methods for the determination of FQs in foods

Sorbent	Sample	Detection method	Main interaction mechanism	LOD (μg kg^{-1})	Recovery (%)	RSD (%)	Number of extra steps for dryness	Ref.
Magnetic graphene	Milk, egg, chicken	HPLC-DAD	Hydrophobic	0.1 (CIP), 0.3 (ENR)	87.4–104.2	4.5–9.7	2	[22]
Zr–Fe–C magnetic nanoparticles	Chicken, beef, turkey meat	HPLC-FLD	Hydrophobic	150 (NOR)	86–111	5–8	0	[23]
One-dimensional polyaniline/magnetic nanoparticles	Honey	HPLC-FLD	Hydrophobic	1.4 (CIP)	86.3–110.1	3.1–11.7	1	[24]
Magnetic PDMS/MWCNTs-OH particles	Honey	CLC-UV	Hydrophobic	0.24 (NOR, CIP), 0.25 (ENR)	84.0–106.0	6.3–7.5	1	[25]
Fe_3O_4@MCM-48 nanocomposite[a]	Pork, fish	HPLC-MS/MS	Hydrophobic	1.0 (NOR), 0.8 (CIP), 0.2 (ENR)	75.3–104.7	2.3–9.0	2	[26]
Fe_3O_4@SiO_2@TZ@Ph magnetic microspheres	Pork	LC-MS/MS	Hydrophobic	0.5 (NOR, CIP, ENR)	81.4–125.7	6.2–10.1	2	[27]
Magnetic MIPs[b]	Milk	HPLC-UV	Hydrophobic	1.8 (CIP)	99.2–124.4	1.5–11.6	1	[28]
Fe_3O_4@CCNs@MIPs	Egg	HPLC-DAD	Hydrophobic	18.4 (CIP)	77.0–81.2	3.2–8.4	1	[29]
PEI-functionalized Fe_3O_4/ATP magnetic particles	Chicken muscle	HPLC-MS/MS	Hydrophilic	0.02 (NOR), 0.08 (CIP), 0.06 (ENR)	83.9–98.7	1.3–6.8	0	This work

CLC capillary liquid chromatography

[a] MCM-48: unique mesoporous molecular sieve material

[b] MIPs: water-compatible commercial MIPs material

Conclusions

Hydrophilic PEI-functionalized Fe_3O_4/ATP magnetic particles were successfully fabricated by a simple co-mixing method for the first time. PEI and Fe_3O_4 magnetic particles were trapped spontaneously on the ATP surface, with good preparation reproducibility. The as-prepared magnetic particles were stable in alkaline solution and could be reused at least 40 times. Thanks to the ATP introduced to the magnetic particles, the maximal adsorption capacity is significantly improved to be 17.33 mg for NOR. Based on the developed magnetic particles, MSPE pretreatment was optimized and combined with RPLC-MS/MS to determine three FQs in chicken muscle samples. This promising method provides low LODs, satisfactory repeatability, high recoveries, and wide linear ranges. Compared with the existing MSPE methods for FQ determination, the sample preparation procedure is simplified by omitting drying steps because of the hydrophilic interaction-based MSPE. It has the potential for applications in the daily monitoring of FQs in food products of animal origin.

Supplementary Information The online version contains supplementary material available at https://doi.org/10.1007/s00216-021-03304-9.

Funding This work was supported by the Zhejiang Province Public Welfare Technology Application Research Project (grant numbers LGC19B050004) and the supports from the Ningbo Natural Science Foundation of China (grant number 202003N4168, 2017A610075), the supports from the National Natural Science Foundation of China (grant number 21405085), the Zhejiang Province Medical and Health Science and Technology Plan Project (grant number 2018KY710), and the Ningbo Public Welfare Science and Technology Plan Project (grant number 2019C50095).

Declarations

Conflict of interest The authors declare that no competing interests.

References

1. Zhang Z, Cheng H. Recent development in sample preparation and analytical techniques for determination of quinolone residues in food products. Crit Rev Anal Chem. 2017;47(3):223–50.
2. Githinji LJM, Musey MK, Ankumah RO. Evaluation of the fate of ciprofloxacin and amoxicillin in domestic wastewater. Water Air Soil Pollut. 2011;219:191–201.
3. Beck R, van Keyserlingk J, Fischer U, Guthoff R, Drewelow B. Penetration of ciprofloxacin, norfloxacin and ofloxacin into the aqueous humor using different topical application modes. Graefes Arch Clin Exp Ophthalmol. 1999;237(2):89–92.
4. Stein GE. Review of the bioavailability and pharmacokinetics of oral norfloxacin. Am J Med. 1987;82(6B):18–21.
5. Tayeb-Cherif K, Peris-Vicente J, Carda-Broch S, Esteve-Romero J. Use of micellar liquid chromatography to analyze oxolinic acid, flumequine, marbofloxacin and enrofloxacin in honey and validation according to the 2002/657/EC decision. Food Chem. 2016;202:316–23.
6. Trouchon T, Lefebvre S. A review of enrofloxacin for veterinary use. Open J Vet Med. 2016;6(2):40–58.
7. Hu Y, Cheng H. Health risk from veterinary antimicrobial use in China's food animal production and its reduction. Environ Pollut. 2016;219:993–7.
8. Hu Y, Cheng H. Use of veterinary antimicrobials in China and efforts to improve their rational use. J Glob Antimicrob Resist. 2015;3(2):144–6.
9. Yang Y, Wang Y, Niu R, Lu J, Zhu X, Wang Y. Preparation and characterization of chitosan microparticles for immunoaffinity extraction and determination of enrofloxacin. Int J Biol Macromol. 2016;93(Pt A):783–8.
10. Zhang X, Wang C, Yang L, Zhang W, Lin J, Li C. Determination of eight quinolones in milk using immunoaffinity microextraction in a packed syringe and liquid chromatography with fluorescence detection. J Chromatogr B. 2017;1064:68–74.
11. da Silva MC, Orlando RM, Faria AF. Electrical field assisted matrix solid phase dispersion as a powerful tool to improve the extraction efficiency and clean-up of fluoroquinolones in bovine milk. J Chromatogr A. 2016;1461:27–34.
12. Sun X, Wang J, Li Y, Yang J, Jin J, Shah SM, et al. Novel dummy molecularly imprinted polymers for matrix solid-phase dispersion extraction of eight fluoroquinolones from fish samples. J Chromatogr A. 2014;1359:1–7.
13. Yan H, Qiao F, Row KH. Molecularly imprinted-matrix solid-phase dispersion for selective extraction of five fluoroquinolones in eggs and tissue. Anal Chem. 2007;79(21):8242–8.
14. Tang Y, Xu J, Chen L, Qiu J, Liu Y, Ouyang G. Rapid in vivo determination of fluoroquinolones in cultured puffer fish (Takifugu obscurus) muscle by solid-phase microextraction coupled with liquid chromatography-tandem mass spectrometry. Talanta. 2017;175:550–6.
15. Pang J, Liao Y, Huang X, Ye Z, Yuan D. Metal-organic framework-monolith composite-based in-tube solid phase microextraction on-line coupled to high-performance liquid chromatography-fluorescence detection for the highly sensitive monitoring of fluoroquinolones in water and food samples. Talanta. 2019;199:499–506.
16. Fan W, He M, Wu X, Chen B, Hu B. Graphene oxide/polyethyleneglycol composite coated stir bar for sorptive extraction of fluoroquinolones from chicken muscle and liver. J Chromatogr A. 2015;1418:36–44.
17. Timofeeva I, Timofeev S, Moskvin L, Bulatov A. A dispersive liquid-liquid microextraction using a switchable polarity dispersive solvent. Automated HPLC-FLD determination of ofloxacin in chicken meat. Anal Chim Acta. 2017;949:35–42.
18. Chen G, Li Q. Luminescence screening of enrofloxacin and ciprofloxacin residues in swine liver after dispersive liquid-liquid microextraction cleanup. J Agric Food Chem. 2013;61(1):98–102.
19. Li H, Yin J, Liu Y, Shang J. Effect of protein on the detection of fluoroquinolone residues in fish meat. J Agric Food Chem. 2012;60(7):1722–7.
20. Janusch F, Scherz G, Mohring SAI, Stahl J, Hamscher G. Comparison of different solid-phase extraction materials for the determination of fluoroquinolones in chicken plasma by LC-MS/MS. J Chromatogr B. 2014;951–952:149–56.
21. Wu X, Wu L. Molecularly imprinted polymers for the solid-phase extraction of four fluoroquilones from milk and lake water samples. J Sep Sci. 2015;38(20):3615–21.
22. He X, Wang GN, Yang K, Liu HZ, Wu XJ, Wang JP. Magnetic graphene dispersive solid phase extraction combining high performance liquid chromatography for determination of fluoroquinolones in foods. Food Chem. 2017;221:1226–31.
23. Vakh C, Alaboud M, Lebedinets S, Korolev D, Postnov V, Moskvin L, et al. An automated magnetic dispersive micro-solid phase extraction in a fluidized reactor for the determination of

fluoroquinolones in baby food samples. Anal Chim Acta. 2018;1001:59–69.
24. Gao Q, Zheng HB, Luo D, Ding J, Feng YQ. Facile synthesis of magnetic one-dimensional polyaniline and its application in magnetic solid phase extraction for fluoroquinolones in honey samples. Anal Chim Acta. 2012;720:57–62.
25. Xu S, Jiang C, Lin YX, Jia L. Magnetic nanoparticles modified with polydimethylsiloxane and multi-walled carbon nanotubes for solid-phase extraction of fluoroquinolones. Microchim Acta. 2012;179:257–64.
26. Yu H, Jia YQ, Wu R, Chen XF, Chan TWD. Determination of fluoroquinolones in food samples by magnetic solid-phase extraction based on a magnetic molecular sieve nanocomposite prior to high-performance liquid chromatography and tandem mass spectrometry. Anal Bioanal Chem. 2019;411(13):2817–26.
27. Xu F, Liu F, Wang C, Wei Y. Use of phenyl/tetrazolyl-functionalized magnetic microspheres and stable isotope labeled internal standards for significant reduction of matrix effect in determination of nine fluoroquinolones by liquid chromatography-quadrupole linear ion trap mass spectrometry. Anal Bioanal Chem. 2018;410(6):1709–24.
28. Zheng HB, Mo JZ, Zhang Y, Gao Q, Ding J, Yu QW, et al. Facile synthesis of magnetic molecularly imprinted polymers and its application in magnetic solid phase extraction for fluoroquinolones in milk samples. J Chromatogr A. 2014;1329:17–23.
29. Wang YF, Wang YG, Ouyang XK, Yang LY. Surface-imprinted magnetic carboxylated cellulose nanocrystals for the highly selective extraction of six fluoroquinolones from egg samples. ACS Appl Mater Interfaces. 2017;9(2):1759–69.
30. Ghanbari D, Salavati-Niasari M. Synthesis of urchin-like CdS-Fe_3O_4 nanocomposite and its application in flame retardancy of magnetic cellulose acetate. J Ind Eng Chem. 2015;24(25):284–92.
31. Gholami T, Salavati-Niasari M, Varshoy S. Investigation of the electrochemical hydrogen storage and photocatalytic properties of $CoAl_2O_4$ pigment: green synthesis and characterization. Int J Hydrog Energy. 2016;41(22):9418–26.
32. Mortazavi-Derazkola S, Salavati-Niasari M, Amiri O, Abbas i A. Fabrication and characterization of Fe_3O_4@SiO_2@TiO_2@Ho nanostructures as a novel and highly efficient photocatalyst for degradation of organic pollution. J Energy Chem. 2017;26(1):17–23.
33. Beshkar F, Khojasteh H, Salavati-Niasari M. Recyclable magnetic superhydrophobic straw soot sponge for highly efficient oil/water separation. J Colloid Interface Sci. 2017;497:57–65.
34. Wang TT, Chen YH, Ma JF, Qian Q, Jin ZF, Zhang LH, et al. Attapulgite nanoparticles-modified monolithic column for hydrophilic in-tube solid-phase microextraction of cyromazine and melamine. Anal Chem. 2016;88(3):1535–41.
35. Chai MS, Chen YH, Xuan RR, Ma JF, Wang TT, Qiu D, et al. Preparation of attapulgite nanoparticles-based hybrid monolithic column with covalent bond for hydrophilic interaction liquid chromatography. Talanta. 2018;189:397–403.
36. Wang TT, Xuan RR, Ma JF, Tan Y, Jin ZF, Chen YH, et al. Using activated attapulgite as sorbent for solid-phase extraction of melamine in milk formula samples. Anal Bioanal Chem. 2016;408(24):6671–7.
37. Xuan RR, Wang TT, Hou CY, Li X, Li Y, Chen YH, et al. Determination of vitamin A in blood serum based on solid-phase extraction using cetyltrimethyl ammonium bromide-modified attapulgite. J Sep Sci. 2019;42(23):3521–7.
38. Song MH, Kim S, Reddy DH, Wei W, Bediako JK, Park S, et al. Development of polyethyleneimine-loaded core-shell chitosan hollow beads and their application for platinum recovery in sequential metal scavenging fill-and-draw process. J Hazard Mater. 2017;324(Pt B):724–31.
39. Chang YC, Chen DH. Preparation and adsorption properties of monodisperse chitosan-bound Fe_3O_4 magnetic nanoparticles for removal of Cu(II) ions. J Colloid Interface Sci. 2005;283(2):446–51.
40. Wang TT, Chen YH, Ma JF, Jin ZF, Chai MS, Xiao XW, et al. A polyethyleneimine-modified attapulgite as a novel solid support in matrix solid-phase dispersion for the extraction of cadmium traces in seafood products. Talanta. 2018;180:254–9.
41. Yang X, Qiao K, Liu F, Wu X, Yang M, Li J, et al. Magnetic mixed hemimicelles dispersive solid-phase extraction based on ionic liquid-coated attapulgite/polyaniline-polypyrrole/Fe_3O_4 nanocomposites for determination of acaricides in fruit juice prior to high performance liquid chromatography-diode array detection. Talanta. 2017;166:93–100.
42. Zang Z, Li Z, Zhang L, Li R, Hu Z, Chang X, et al. Chemically modified attapulgite with asparagine for selective solid-phase extraction and preconcentration of Fe(III) from environmental samples. Anal Chim Acta. 2010;663(2):213–7.
43. Corazzari I, Nisticò R, Turci F, Faga MG, Franzoso F, Tabasso S, et al. Advanced physico-chemical characterization of chitosan by means of TGA coupled on-line with FTIR and GCMS: thermal degradation and water adsorption capacity. Polym Degrad Stab. 2015;112:1–9.
44. Mu B, Wang A. One-pot fabrication of multifunctional superparamagnetic attapulgite/Fe_3O_4/polyaniline nanocomposites served as an adsorbent and catalyst support. J Mater Chem A. 2015;3:281–9.
45. Alpert AJ. Hydrophilic-interaction chromatography for the separation of peptides, nucleic acids and other polar compounds. J Chromatogr. 1990;499:177–96.
46. Kolaei M, Dashtian K, Rafiee Z, Ghaedi M. Ultrasonic-assisted magnetic solid phase extraction of morphine in urine samples by new imprinted polymer-supported on MWCNT-Fe_3O_4-NPs: central composite design optimization. Ultrason Sonochem. 2016;33:240–8.
47. Chai MS, Chen YH, Xuan RR, Ma JF, Jin ZF, Wang TT, et al. Application of polyethyleneimine-modified attapulgite for the solid-phase extraction of chlorophenols at trace levels in environmental water samples. Anal Bioanal Chem. 2018;410(25):6643–51.
48. Wang TT. Polyethyleneimine-modified hybrid silica sorbent for hydrophilic solid-phase extraction of thyreostats in animal tissues. J Chromatogr A. 2018;1581–1582:16–24.
49. Liu H, Li N, Liu X, Qian Y, Qiu J, Wang X. Poly(N-acryloylglucosamine-co-methylenebisacrylamide)-based hydrophilic magnetic nanoparticles for the extraction of aminoglycosides in meat samples. J Chromatogr A. 1609;2020:460517.
50. Guo Y, Gaiki S. Retention behavior of small polar compounds on polar stationary phases in hydrophilic interaction chromatography. J Chromatogr A. 2005;1074(1–2):71–80.
51. Talebi M, Arrua RD, Gaspar A, Lacher NA, Wang Q, Haddad PR, et al. Epoxy-based monoliths for capillary liquid chromatography of small and large molecules. Anal Bioanal Chem. 2013;405(7):2233–44.
52. Chang Y, Lv X, Zha F, Wang Y, Lei Z. Sorption of p-nitrophenol by anion-cation modified palygorskite. J Hazard Mater. 2009;168(2–3):826–31.
53. Chu G, Cai W, Shao X. Preparation of 4-butylaniline-bonded attapulgite for pre-concentration of bisphenol A in trace quantity. Talanta. 2015;136:29–34.
54. Frenich AG, Romero-González R, Gómez-Pérez ML, Vidal JL. Multi-mycotoxin analysis in eggs using a QuEChERS-based extraction procedure and ultra-high-pressure liquid chromatography coupled to triple quadrupole mass spectrometry. J Chromatogr A. 2011;1218(28):4349–56.

Publisher's note Springer Nature remains neutral with regard to jurisdictional claims in published maps and institutional affiliations.